Bloch oscillations in a periodic lattice under a strong (artificial) magnetic field

MARCO COMINOTTI[1,2] and IACOPO CARUSOTTO[1,3]

[1] *Università di Trento, Dipartimento di Fisica, via Sommarive 14, 38123 Povo, Italy*
[2] *Université Grenoble 1/CNRS, Laboratoire de Physique et de Modélisation des Milieux Condensés (UMR 5493), B.P. 166, 38042 Grenoble, France*
[3] *INO-CNR BEC Center and Dipartimento di Fisica, Università di Trento, via Sommarive 14, 38123 Povo, Italy*

PACS 67.85.-d – Ultracold gases, trapped gases
PACS 03.65.Vf – Phases: geometric, dynamic or topological
PACS 73.43.-f – Quantum Hall effects

Abstract –Inspired by recent developments of artificial gauge fields for atoms and for photons, we study the semiclassical dynamics of a quantum particle in a two-dimensional square lattice, under the effect of crossed electric and magnetic fields. We provide an elementary derivation of how the Berry curvature of the Bloch bands modifies the usual semiclassical equations of motion. We then calculate the real-space trajectories of a wave packet and observe that the contribution of this anomalous Berry term can be as important as the usual group velocity one. The connection with the classical Hall effect is finally clarified.

In spite of its simple formulation, the coherent dynamics of a single quantum particle trapped in a periodic lattice potential and subject to a strong magnetic field displays a remarkably rich physics and is responsible for several important effects of condensed-matter physics. While the weak magnetic field case is successfully described by the semiclassical theory of Bloch electron as presented in solid-state physics textbooks [1], magnetic field strengths on the order of one magnetic flux per unit cell of the lattice are responsible for qualitatively novel behaviours. On one hand, pioneering work by Hofstadter [2] has anticipated that the Bloch bands of the lattice are split into many subbands with a fractal structure in the energy vs. magnetic field plane. On the other hand, new terms proportional to the Berry curvature have to be included in the semiclassical theory of transport to account for the peculiar topological properties of the Hofstadter bands [3, 4].

While many consequences of this physics are nowadays known and well understood at a macroscopic level, much less experimental literature is available on microscopic studies of the basic mechanisms: in ordinary solids, huge magnetic fields are required to observe this physics and many spurious decoherence phenomena may compete with the quantum transport. Only recently, the experimental advances in the generation of strong *artificial gauge fields* for (neutral) atoms [5] and for photons [6] are opening new directions in the study of the quantum dynamics under strong magnetic fields: first examples in this direction are the observation of quantized vortices under the effect of a artificial gauge field in an atomic condensate [7] and the study of topologically protected photonic edge states in photonic crystals [8].

In this work we report a theoretical study of Bloch oscillations [9, 10] of a quantum particle trapped in a two-dimensional periodic potential and subject to a strong magnetic field orthogonal to the plane of the lattice. Under the effect of a weak in-plane electric field, the particle performs a slow motion across the magnetic Brillouin zone that reflects in a peculiar real-space trajectory determined not only by the energy dispersion of the band, but also by the Berry curvature of the corresponding eigenstates. Recently, a similar physics was investigated in [11, 12] for atomic lattices of different geometries. In this work, we provide an elementary derivation of the Berry curvature terms and we give a complete discussion of the square lattice case; some interesting features of the connection with the classical Hall physics in free space are also clarified.

The model. – We consider a particle confined in a two-dimensional square lattice of spacing a, immersed in

a uniform artificial magnetic field $\mathbf{B} = B\hat{z}$ perpendicular to the xy plane of the lattice [1]. Within the Landau gauge, the vector potential associated to the uniform magnetic field $\mathbf{B}$ has the form $\mathbf{A}(\mathbf{r}) = Bx\hat{y}$.

Within a standard tight-binding (TB) approximation for the periodic lattice potential, the single particle Hamiltonian can be written in the Peierls form

$$H = -J \sum_{\langle i,j \rangle} \hat{a}_i^\dagger \hat{a}_j e^{i\phi_{ij}} \,, \tag{1}$$

as the sum of hopping terms between neighboring sites with a non-trivial phase of the hopping amplitude. Here, the indices i and j indicate the lattice site, and the sum is restricted only to the nearest-neighboring sites. The $\hat{a}_i^\dagger$ ($\hat{a}_i$) operators create (annihilate) one particle at the lattice site i and satisfy usual bosonic commutation rules $[\hat{a}_i, \hat{a}_j^\dagger] = \delta_{i,j}$.

J is a real and positive coefficient quantifying the strength of tunneling and the phase of the hopping amplitude from site j to site i can be written in terms of a line integral of the vector potential along the hopping path $\mathbf{r}_j \to \mathbf{r}_i$,

$$\phi_{ij} = -\frac{e}{\hbar} \int_{\mathbf{r}_j}^{\mathbf{r}_i} \mathbf{A}(\mathbf{r}) \cdot \mathrm{d}\mathbf{r} \,. \tag{2}$$

While the hopping phase along a single link of the lattice is manifestly not gauge invariant, the sum of the phases accumulated while hopping around a closed contour is gauge invariant and proportional to the magnetic field flux encircled by the contour in units of the flux quantum $\phi_0 = e/2\pi\hbar$. The key parameter determining the properties of the model is then α, defined in terms of the number of magnetic flux quanta across the elementary cell of the lattice as

$$\alpha = \frac{\phi}{\phi_0} = -\frac{1}{2\pi} \sum_{\square} \phi_{ij} = \frac{e}{2\pi\hbar} B a^2 \,. \tag{3}$$

In the Landau gauge used in this work, the hopping amplitude along the x direction has a phase $\phi_{ij}^{\hat{x}} = 0$, while the one along the y direction has a phase $\phi_{ij}^{\hat{y}} = -eBax/\hbar$.

The band structure. – Even though the application of a uniform magnetic field does not affect the (discrete) translational symmetry of the physical system, this is not apparent in the Hamiltonian (1) where the hopping amplitudes have a spatially dependent phase stemming from the spatial dependence of the vector potential $\mathbf{A}$. Of course, this breaking of the translational symmetry is only fictitious, as it is exactly compensated by a suitable gauge transformation.

To diagonalize the Hamiltonian (1), it is useful to consider the so-called *magnetic translation group* [13, 14], whose operators $\tilde{T}_{\mathbf{a}}$ are defined as

$$\tilde{T}_{\mathbf{a}} = e^{-ie\Delta\mathbf{A}_{\mathbf{a}}(\mathbf{r})\cdot\mathbf{r}/\hbar}\, T_{\mathbf{a}} \tag{4}$$

in terms of the usual lattice translation operators $T_{\mathbf{a}}$ and of the vector potential variation $\Delta\mathbf{A}_{\mathbf{a}}(\mathbf{r}) = \mathbf{A}(\mathbf{r}+\mathbf{a}) - \mathbf{A}(\mathbf{r})$. A complete mathematical characterization of the magnetic translation group is given in [15, 16]. Here, it is enough to note that all $\tilde{T}_{\mathbf{a}}$ commute with the Hamiltonian H in (1) but they do not in general commute among them. For instance, the magnetic translation operators for the two unit lattice vectors $\mathbf{a}_{x,y}$ in the x, y directions satisfy

$$\tilde{T}_{\mathbf{a}_x} \tilde{T}_{\mathbf{a}_y} = \tilde{T}_{\mathbf{a}_y} \tilde{T}_{\mathbf{a}_x} e^{-2\pi i\alpha} \;: \tag{5}$$

commutation of $\tilde{T}_{\mathbf{a}_x}$ and $\tilde{T}_{\mathbf{a}_y}$ is satisfied only if the magnetic flux through a plaquette is an integer multiple of the flux quantum ϕ_0. On the other hand, for a rational $\alpha = p/q$ (with p, q co-prime integers), it is possible to define a larger *magnetic unit cell* as the union of q adjacent lattice plaquettes: the magnetic flux through the magnetic unit cell is then an integer multiple of ϕ_0, but the wider spatial periodicity corresponds to a q times smaller magnetic Brillouin zone (MBZ). While the choice of the magnetic unit cell is not unique in general, we can take for simplicity a magnetic unit cell formed by q adjacent plaquettes along the $\hat{x}$ direction. With this choice, the MBZ becomes of rectangular shape $[-\pi/qa, \pi/qa] \times [-\pi/a, \pi/a]$, with a shorter size along $\hat{k}_x$.

Since the Hamiltonian H in (1) commutes with the magnetic translation operators, we can look for the common eigenstates, which we will call *magnetic Bloch states*. To conserve the total number of states, the reduced size of the magnetic Brillouin zone will be compensated by the single tight-binding band of the non-magnetic $\alpha = 0$ system being folded into q magnetic bands. This was first done by Hofstaedter [2] who reduced the problem to the solution of a one-dimensional difference equation, the so-called Harper equation [17]:

$$\begin{aligned} &- J\,[g(m+1) + g(m-1)] \\ &\qquad - 2J\,\cos(2\pi\alpha m - k_y) g(m) = \mathcal{E} g(m) \,. \end{aligned} \tag{6}$$

Here, the spatial coordinates x and y have been discretized on the lattice points as $x = ma$, $y = na$, with $m, n \in \mathbb{Z}$. Thanks to the discrete translational symmetry along the $\hat{y}$ direction of the vector potential in the chosen Landau gauge, a plane wave form can be assumed for the eigenfunction $\psi(m,n)$ along the $\hat{y}$ direction, $\psi(m,n) = \exp(ik_y n) g(m)$.

Even though the eigenvalues of the Hamiltonian (1) arrange in a very complex fractal structure in the energy E vs. magnetic field parameter α, the so-called *Hofstadter butterfly*, exciting physics is obtained in the case of a rational $\alpha = p/q$ where the effective potential appearing in the Harper equation (6) is periodic in the $\hat{x}$ direction with a period of q lattice points, in agreement with the magnetic translation arguments.

In particular, for each value of k_y, the eigenstates of the Harper equation are then classified according to the Bloch theorem in terms of a k_x wavevector contained in

[1] As we are dealing with artificial gauge fields, only the products $e\mathbf{E}$ and $e\mathbf{B}$ have a physical meaning.

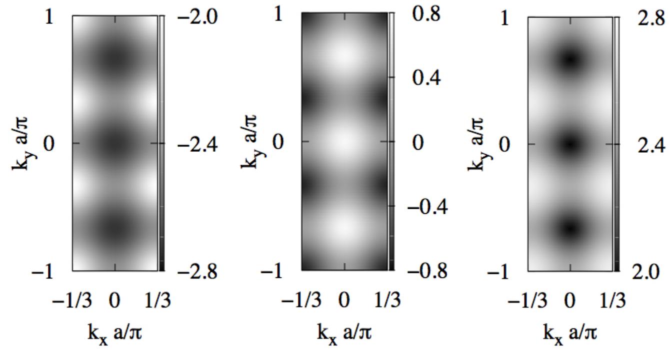

Fig. 1: Energy dispersion of the three magnetic bands in the $\alpha = 1/3$ case in units of the tunneling energy J.

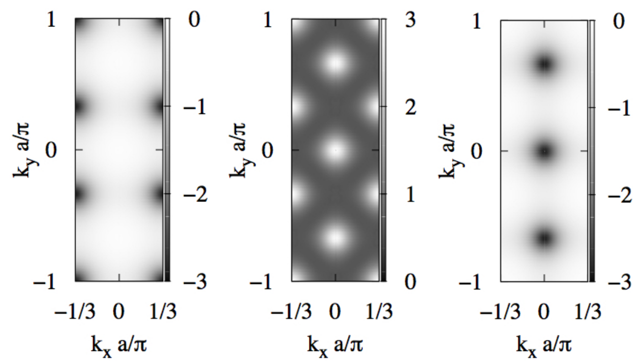

Fig. 2: Normalized Berry curvature $\mathbf{\Omega}_n/a^2$ of the three magnetic bands in the $\alpha = 1/3$ case. The three panels refer to the corresponding panels in Fig.1. We have numerically checked that upon integration over the whole MBZ, the Chern numbers for the three bands are respectively $C_n = -1, 2, -1$.

$[-\pi/qa, \pi/qa]$. As a result, we can classify the eigenstates of the Hamiltonian (1) in terms of $k_{x,y}$ within the magnetic Brillouin zone and plot the resulting magnetic bands. In the non-magnetic $\alpha = 0$ case, one recovers the standard cosine shape of the tight-binding energy band, $\mathcal{E} = -2J\,[\cos(k_x) + \cos(k_y)]$. In the more interesting $\alpha = 1/3$ case, the three bands have a non-trivial structure as shown in Fig. 1. In particular, note the additional q-fold periodicity of the Hofstadter bands in the y direction.

For decreasing values of $\alpha = 1/q$, the standard physics of the Landau levels is recovered in that the q bands become flatter and flatter and the spacing of the lower ones tends to the cyclotron frequency $\omega_c = eB/m$. This behavior can be recovered from the Harper equation (6) as follows: for $q \to \infty$, the minima of the oscillating potential becomes widely separated in space, so tunneling between them is suppressed. As the oscillating potential becomes smoother, the spacing between the eigenstates decreases and the lowest states end up exploring the harmonic bottom only. More details on this physics will be discussed in the last section of the Letter in connection with the classical Hall effect.

Semiclassical dynamics. – In the previous section, we have studied the eigenstates of the particle motion in the presence of a uniform magnetic field: in particular, we have seen that they are classified in terms of a $\mathbf{k}$ vector within the MBZ. Within a semiclassical picture, we now proceed to study the spatial motion of a particle in terms of the time evolution of a wave packet contained within the n-th magnetic band and localized (as much as the Heisenberg principle allows it, of course) in both real and $\mathbf{k}$ space around $\mathbf{r}_c$ and $\mathbf{k}_c$, respectively.

According to the modern semiclassical theory of electron transport in solids [3, 4], the time evolution of the wavepacket center of mass $\mathbf{r}_c$ and $\mathbf{k}_c$ is ruled by the following pair of equations,

$$\hbar\dot{\mathbf{k}}(t) = e\mathbf{E}\,, \tag{7a}$$
$$\hbar\dot{\mathbf{r}}_n(t) = \nabla_{\mathbf{k}}\mathcal{E}_{n,\mathbf{k}} - e\mathbf{E}\times\mathbf{\Omega}_n(\mathbf{k})\,. \tag{7b}$$

The first Eq.(7a) describes the usual evolution of the (quasi-)momentum under the effect of the electric force $e\mathbf{E}$, as discussed in solid-state textbooks [1]. Of course, accuracy of the semiclassical theory requires that this force is weak enough not to induce Landau-Zener interband transitions.

The second Eq.(7b) is much more interesting: while the first term recovers the usual group velocity $\mathbf{v}^{\rm gr}_{n,\mathbf{k}} = \frac{1}{\hbar}\nabla_{\mathbf{k}}\mathcal{E}_{n,\mathbf{k}}$ of a particle living on the energy band $\mathcal{E}_{n,\mathbf{k}}$, the second term involves the so-called Berry curvature of the band, geometrically introduced as the curvature

$$\mathbf{\Omega}_n(\mathbf{k}) = \nabla_{\mathbf{k}}\times\mathcal{A}_{n,\mathbf{k}} \tag{8}$$

of the Berry connection

$$\mathcal{A}_{n,\mathbf{k}} = i\langle u_{n,\mathbf{k}}|\nabla_{\mathbf{k}}u_{n,\mathbf{k}}\rangle\,, \tag{9}$$

defined in terms of the periodic part $u_n(\mathbf{k})$ of the Bloch wavefunction $\psi_{n,\mathbf{k}}(\mathbf{r}) = \exp(i\mathbf{k}\cdot\mathbf{r})\,u_{n,\mathbf{k}}(\mathbf{r})$. This second contribution is the so-called anomalous or Berry velocity, which provides a spatial drift proportional to the temporal variation of the $\mathbf{k}$ vector, and directed orthogonally to the applied force. In the solid-state context, this extra contribution to the velocity of the electrons was first noticed by Karplus and Luttinger [18] in the framework of a linear response analysis. More recently, it has been reinterpreted in a more general framework as a Berry phase effect in [3, 4]. An elementary derivation is sketched in the next section.

Physically, the most striking consequence of Eqs. (7) is that the semiclassical dynamics is not completely encoded in the energy spectrum of the Hamiltonian, but keeps track

of the relative phase of the eigenstates via their Berry curvature (8). While the Berry curvature identically vanishes for systems with simultaneous time-reversal and spatial inversion symmetries, a non-trivial value of $\mathbf{\Omega}_{n,\mathbf{k}}$ stems in our case from the presence of the external magnetic field breaking time-reversal.

A plot of the Berry curvature for the three magnetic bands in the $\alpha = 1/3$ case is shown in Fig.2: its general structure reflects the q-fold degeneracy of the energy bands in the k_y direction. Thanks to the inversion symmetry of the system, the curvature is symmetric under $\mathbf{k} \to -\mathbf{k}$. Finally, the sum of the Berry curvature of the different bands at the same point $\mathbf{k}$ in momentum space identically vanishes throughout the whole MBZ.

The most celebrated consequence of the Berry curvature in electron transport is the Hall effect, in particular the so-called integer quantum Hall effect: the quantized value of the Hall conductivity can be related to the *Chern number* of the occupied bands, an integer-valued topological invariant defined as the integral of the Berry curvature over the magnetic Brillouin zone in units of 2π [19]. Other electronic systems displaying bands with non-trivial Berry curvature are ferromagnetic Fe crystals [20] or graphene single layers with a staggered potential breaking the spatial inversion [12, 21].

Elementary derivation of the anomalous Berry velocity. – Before proceeding, it is worth presenting an elementary derivation of the semiclassical equations of motions that does not rely on the Lagrangian formalism used in the original works [3, 4]. For simplicity, we restrict to the simplest case of a weak and constant electric field $\mathbf{E}$. With a suitable choice of gauge, both the magnetic and the electric fields can be included in a (slowly varying) vector potential

$$\mathbf{A}(\mathbf{r}, t) = \mathbf{A_B}(\mathbf{r}) - \mathbf{E}\, t, \tag{10}$$

the first constant term $\mathbf{A_B}(\mathbf{r})$ referring to the constant magnetic field, $\nabla \times \mathbf{A_B} = \mathbf{B}$. The system Hamiltonian $\bar{H}(t)$ will have again the same form (1) but the hopping phases defined by (2) in terms of the vector potential (10) will be now time-dependent. The Hamiltonian $\bar{H}(t)$ has the same magnetic translation symmetry properties as the Hamiltonian (1) and the eigenstates can be classified in terms of the momentum $\mathbf{k}$ within the MBZ. Provided the temporal variation $\mathbf{A}(t)$ is slow enough, the adiabatic theory guarantees that no inter-band transition will occur. Thanks to the magnetic translational symmetry of $\bar{H}$, each $\mathbf{k}$ component will be decoupled from all others and will just acquire a $\mathbf{k}$-dependent phase factor.

Under this approximation, the semiclassical state will be written in the form

$$|W(t)\rangle = \int \mathrm{d}^2\mathbf{k}\, w(\mathbf{k}) |\bar{\psi}^{(t)}_{n,\mathbf{k}}\rangle\,, \tag{11}$$

where $|\bar{\psi}^{(t)}_{n,\mathbf{k}}\rangle$ is the eigenstate of the Hamiltonian $\bar{H}(t)$ at a wavevector $\mathbf{k}$ on the magnetic band n of interest at time t. During time-evolution, the eigenfunctions of the Hamiltonian acquires a $\mathbf{k}$-dependent phase $\theta(\mathbf{k}, t)$, according to Berry's adiabatic theorem, satisfying

$$\hbar \frac{\partial}{\partial t} \theta(\mathbf{k}, t) = -\bar{\mathcal{E}}^{(t)}_{n,\mathbf{k}} + e\mathbf{E} \cdot \bar{\mathcal{A}}^{(t)}_{n,\mathbf{k}}\,, \tag{12}$$

in terms of the eigenenergy $\mathcal{E}^{(t)}_{n,\mathbf{k}}$ of $\bar{H}(t)$ at the given time t. The physical meaning of the Berry term

$$\bar{\mathcal{A}}^{(t)}_{n,\mathbf{k}} = i \langle \bar{\psi}^{(t)}_{n,\mathbf{k}} | \frac{\partial \bar{\psi}^{(t)}_{n,\mathbf{k}}}{\partial t} \rangle \tag{13}$$

becomes transparent once we note that the eigenstate of the time-dependent $\bar{H}(t)$ at wavevector $\mathbf{k}$ coincides with the one at wavevector $\mathbf{k} + e\mathbf{E}t$ of the original Hamiltonian $H = \bar{H}(0)$ as defined in (1), $\bar{\mathcal{E}}^{(t)}_{n,\mathbf{k}} = \mathcal{E}^{(t)}_{n,\mathbf{k}+e\mathbf{E}t}$ and $|\bar{\psi^{(t)}}_{n,\mathbf{k}}\rangle = |\psi^{(t)}_{n,\mathbf{k}+e\mathbf{E}t}\rangle$. This can be easily shown by means of a gauge transformation to eliminate the time-dependent component of the vector potential. Analogously, the Berry term is related to the usual Berry connection on the MBZ by $\bar{\mathcal{A}}_{n,\mathbf{k}} = \mathcal{A}_{n,\mathbf{k}+e\mathbf{E}t}$.

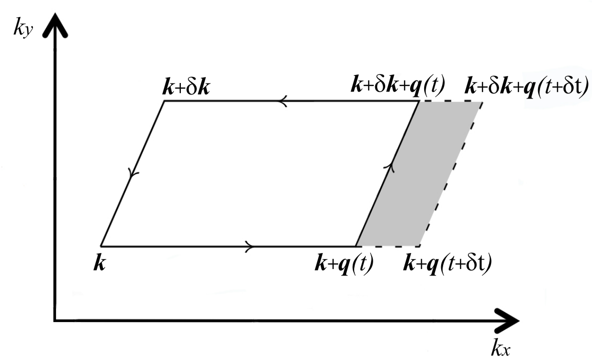

Fig. 3: Sketch of the integration paths involved in the time evolution of the phase $\theta(\mathbf{k}, t)$. We indicate $\mathbf{q}(t) = e\mathbf{E}t$.

To obtain the evolution equation for the real space position $\mathbf{r}_c$ of the wavepacket, it is then enough to apply the stationary-phase approximation to the wavefunction (11) using the form (12) of the phase. Under this approximation, the position $\mathbf{r}_c$ is determined by the $\mathbf{k}$-gradient of the phase $\theta(\mathbf{k}, t)$ as

$$\mathbf{r}_c = -\nabla_{\mathbf{k}} \left[\mathrm{Arg}[w(\mathbf{k})] + \theta(\mathbf{k}, t) + \mathcal{A}_{n,\mathbf{k}+e\mathbf{E}t} \right]\,, \tag{14}$$

note in particular the non-trivial term proportional to the Berry connection $\mathcal{A}$ that accounts for the $\mathbf{k}$-dependence of the phase of the Bloch eigenstate. The equation for the velocity $\mathrm{d}\mathbf{r}_c/\mathrm{d}t$ is then obtained as a time derivative

$$\frac{\mathrm{d}\mathbf{r}_c}{\mathrm{d}t} = \mathbf{v}^{\mathrm{gr}}_{n,\mathbf{k}} - \frac{e}{\hbar} \mathbf{E} \times \mathbf{\Omega}_{n,\mathbf{k}}\,, \tag{15}$$

the first term is a direct consequence of the definition $\mathbf{v}^{\mathrm{gr}}_{n,\mathbf{k}} = \frac{1}{\hbar} \nabla_{\mathbf{k}} \mathcal{E}_{n,\mathbf{k}}$. The term involving the Berry curvature requires a bit more care and can be intuitively understood

from the sketch in Fig.3: the difference of the phases θ acquired after a time t by the components of wavevectors $\mathbf{k}$ and $\mathbf{k}+\delta\mathbf{k}$ is given by the difference of the integrals of the Berry connection $\mathcal{A}$ taken along the two horizontal sides of the parallelogram. The variation of the Berry connection term in (14) corresponds instead to the difference of the integral of the Berry connection taken along the two shorter sides. The sum of all these contributions recovers the time-derivative of the integral of the Berry connection around the whole parallelogram, that is the flux of the Berry curvature through the infinitesimal gray-shaded area,

$$\frac{1}{\delta t}[\mathbf{E}\,\delta t \times \delta\mathbf{k}] \cdot \mathbf{\Omega} = -(\mathbf{E} \times \mathbf{\Omega}) \cdot \delta\mathbf{k}. \qquad (16)$$

Magnetic Bloch oscillations. – A most fascinating feature of the quantum dynamics of a particle in a periodic lattice are the so-called *Bloch oscillations* (BO), that is a periodic motion in both real and momentum space under the effect of a uniform and time-independent force. In the solid-state context, scattering and dephasing effects due to impurities in the crystal and to interaction with phonons make the observation of BO's in ordinary solids extremely difficult unless artificial superlattices with enhanced nm periodicities are used [9]. On the other hand, the extremely clean periodic potential experienced by atoms in optical lattices has allowed for a neat observations of BO's, mostly in momentum space [10,22,23]. Very recently, this same effect has been exploited to map the band structure of atoms in a honeycomb-like lattice potential [24].

Starting from the semiclassical Eq.(7a), the oscillation frequency along each principal direction x, y of the lattice is proportional to the corresponding component $eE_{x,y}$ of the applied force, $\omega_B^{(x,y)} = eE_{x,y}a/2\pi\hbar$: the momentum $\mathbf{k}$ wraps around the FBZ at a constant speed set by the applied force; whenever it reaches an edge of the FBZ, a Bragg scattering process makes it to reappear on the other side.

Under the same semiclassical approximation, the spatial motion is ruled by Eq.(7b): in standard lattices with zero Berry curvature $\mathbf{\Omega} = 0$, the shape of the BO is fully determined by the group velocity term. In the simplest case where the force is directed along a principal axis and the momentum starts from a high symmetry point like $\mathbf{k} = 0$, the BO have the usual back-and-forth shape along the direction of the force and their spatial amplitude is $\Delta x = \Delta\mathcal{E}/|e\mathbf{E}|$ where $\Delta\mathcal{E}$ is the width of the energy band explored by the particle momentum along its path across the FBZ. In the general case, the complicate shape of the band energy $\mathcal{E}_{n,\mathbf{k}}$ across the FBZ leads to complex trajectories in real space, which do not typically close on themselves and can show lateral drifts [25].

The situation is far more interesting in the presence of a finite magnetic field $\alpha > 0$. To concentrate on the physics of interest, we again start from the high symmetry $\mathbf{k} = 0$ point in $\mathbf{k}$-space and we direct the applied force along the symmetry direction $\hat{x}$: as a result, the wave vector $\mathbf{k}$ sweeps the MBZ along the $k_y = 0$ line and the group velocity remains by symmetry always directed along x. Still, as it is illustrated in Fig.4 the particle motion from the initial position $\mathbf{r} = 0$ shows a non-vanishing drift along the y direction due to the Berry curvature in addition to the periodic Bloch oscillation along x: the different curves show these magnetic Bloch oscillations (MBO) for each of the three magnetic bands of the $\alpha = 1/3$ case, whose Berry curvatures differ in both magnitude and sign. The relative amplitude of the motion along x and y is determined by the strength of the applied force $\mathbf{E}$: the stronger this force, the shorter the amplitude of the periodic motion along x and the more important the lateral drift term in the y direction.

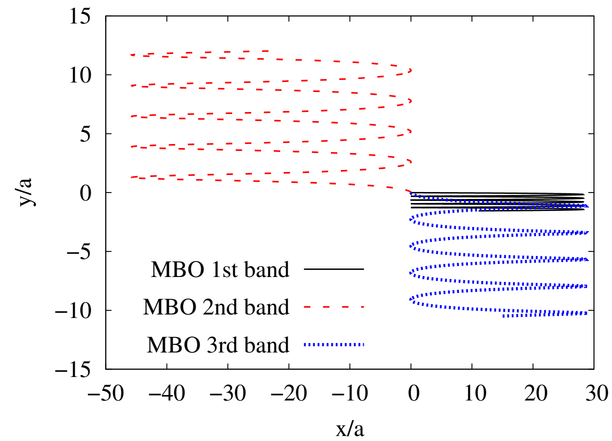

Fig. 4: Trajectory of the magnetic Bloch oscillations (MBO) in the $\alpha = 1/3$ case. The applied electric field is in the $\hat{x}$ direction and has a strength $0.01\ J/a$. The starting point of the MBO is at the origin of both real and reciprocal spaces, $\mathbf{r} = 0$, $\mathbf{k} = 0$.

In the general case of an arbitrary initial wavevector $\mathbf{k}$, the trajectory of the MBO is much more complicate, which makes it difficult to isolate the contribution of the Berry curvature. A clever time-reversal protocol to overcome this difficulty and obtain a complete mapping of the Berry curvature over the whole MBZ was proposed in [12].

Low magnetic field regime and Hall effect. – In order to make our discussion complete, it is interesting to see how the classical Hall effect for a charged particle in free space under crossed electric and magnetic fields is recovered in our formalism. In order to recover this physics in the lattice model, it is enough to let the lattice spacing $a \to 0$ at constant values of the effective mass $m^* = \hbar^2/2Ja^2$ and of the applied electric $\mathbf{E}$ and magnetic $\mathbf{B}$ fields. In this limit, the discreteness of the lattice should disappear and the system should recover the textbook classical mechanics prediction: the particle motion follows a cycloidal trajectory resulting from the superposition of a circular motion at the cyclotron frequency $\omega_c = eB/m$ and a uniform drift at a Hall velocity

$$\mathbf{v}_H = -\mathbf{E} \times \mathbf{B}/B^2. \qquad (17)$$

In a most important limiting case, the circular motion degenerates into a point and one is left with only the uniform drift at the Hall velocity $\mathbf{v}_H$.

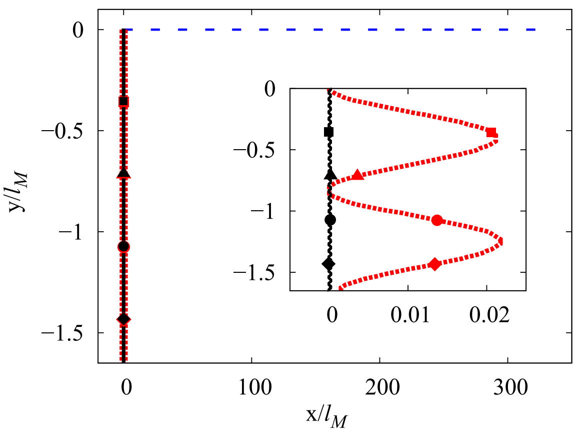

Fig. 5: Real-space trajectories (measured in units of the magnetic length $l_M = \sqrt{\hbar/eB}$) of a particle under crossed electric and magnetic fields for a magnetic field strength $\alpha = 1/9$. The black solid line is the classical trajectory in free space for an initial condition such that the circular component of the motion degenerates to a single point. The red dashed line is the MBO in the lowest magnetic band. Corresponding symbols on top of each trajectory indicate the positions at corresponding times. The blue dashed line is the BO trajectory for vanishing magnetic field $\alpha = 0$. The inset is a magnified view of the region close to $x = 0$.

In Fig.5 we show how this behavior is recovered in our quantum mechanical lattice model. For low values of the magnetic field strength α, the lowest magnetic energy bands typically flatten tending to a series of equispaced Landau levels separated by the cyclotron frequency ω_c in the $\alpha \to 0$ limit. Correspondingly, also the Berry curvature Ω_0 of the lowest band tends to a constant across the whole FBZ. Approximating Ω_0 with a constant and knowing that the Chern number of this band is $C_0 = -1$, one can heuristically determine its value to $\mathbf{\Omega}_0 = -\hbar\hat{z}/eB$. Inserting these remarks into the second semiclassical equation Eq.(7b), one immediately sees that the flatness of the bands reflects into a very small amplitude of the MBO, while the Berry curvature term recovers the drift at the Hall velocity $\mathbf{v}_H$: it is quite remarkable to see that to recover the Hall effect in the quantum mechanical lattice model one has to properly keep into account the Berry curvature! The small-sized MBO that are visible in the inset are due to the exponentially small, but still finite width of the magnetic bands: it is important to note that their frequency is determined by the strength E of the applied electric field and are distinct from the cyclotron motion of classical mechanics, whose frequency is determined by the strength B of the magnetic field. For this latter to be recovered in the quantum picture, one should in fact take as the initial state of the particle a linear superposition of the different magnetic bands, that are indeed spaced by the cyclotron frequency ω_c.

Conclusions. – We have studied the semiclassical dynamics of a quantum mechanical particle in a two-dimensional lattice in the presence of a strong (artificial) magnetic field. Under a constant (artificial) electric field, the main effect of the Berry curvature of the magnetic bands is to introduce a lateral drift in addition to the periodic Bloch oscillations along the electric field direction. An explicit derivation of this result is presented in terms of elementary quantum mechanics. In the continuum limit, the amplitude of the Bloch oscillations tends to zero, while the lateral drift due to the Berry curvature recovers the classical Hall velocity in crossed electric and magnetic fields.

* * *

We thank R. O. Umucalilar for useful discussions.

REFERENCES

[1] Ashcroft N. W. and Mermin N. D., *Solid State Physics* (Brooks/Cole) 1976.
[2] Hofstadter D. R., *Phys. Rev. B*, **14** (1976) 2239.
[3] Chang M.-C. and Niu Q., *Phys. Rev. B*, **53** (1996) 7010.
[4] Sundaram G. and Niu Q., *Phys. Rev. B*, **59** (1999) 14915.
[5] Dalibard J., Gerbier F., Juzeliūnas G. and Öhberg P., *Rev. Mod. Phys.*, **83** (2011) 1523.
[6] Carusotto I. and Ciuti C., *Rev. Mod. Phys.*, (2013) . `http://arxiv.org/abs/1205.6500`
[7] Lin Y. J., Compton R. L., Jimenez-Garcia K., Porto J. V. and Spielman I. B., *Nature*, **462** (2009) 628.
[8] Wang Z., Chong Y. D., Joannopoulos J. D. and Soljačić M., *Phys. Rev. Lett.*, **100** (2008) 013905.
[9] Leo K., Bolivar P. H., Brggemann F., Schwedler R. and Khler K., *Solid State Communications*, **84** (1992) 943 .
[10] Ben Dahan M., Peik E., Reichel J., Castin Y. and Salomon C., *Phys. Rev. Lett.*, **76** (1996) 4508.
[11] Dudarev A. M., Diener R. B., Carusotto I. and Niu Q., *Phys. Rev. Lett.*, **92** (2004) 153005.
[12] Price H. M. and Cooper N. R., *Phys. Rev. A*, **85** (2012) 033620.
[13] Lifshitz E. M. and Pitaevskii L., *Statistical Physics, Part 2* Vol. 9 of *Course of Theoretical Physics* (Butterworth-Heinemann) 1980.
[14] Xiao D., Chang M.-C. and Niu Q., *Rev. Mod. Phys.*, **82** (2010) 1959.
[15] Zak J., *Phys. Rev.*, **134** (1964) A1602.
[16] Zak J., *Phys. Rev.*, **134** (1964) A1607.
[17] Harper P. G., *Proc. Phys. Soc.A*, **68** (1955) 874.
[18] Karplus R. and Luttinger J. M., *Phys. Rev.*, **95** (1954) 1154.
[19] Thouless D. J., Kohmoto M., Nightingale M. P. and den Nijs M., *Phys. Rev. Lett.*, **49** (1982) 405.

[20] Yao Y., Kleinman L., MacDonald A. H., Sinova J., Jungwirth T., Wang D.-s., Wang E. and Niu Q., *Phys. Rev. Lett.*, **92** (2004) 037204.
[21] Zhou S. Y., Gweon G.-H., Fedorov A. V., First P. N., de Heer W. A., Lee D.-H., Guinea F., Castro Neto A. H. and Lanzara A., *Nature Materials*, **6** (2007) 770.
[22] Roati G., de Mirandes E., Ferlaino F., Ott H., Modugno G. and Inguscio M., *Phys. Rev. Lett.*, **92** (2004) 230402.
[23] Cristiani M., Morsch O., Müller J. H., Ciampini D. and Arimondo E., *Phys. Rev. A*, **65** (2002) 063612.
[24] Tarruell L., Greif D., Uehlinger T., Jotzu G. and Esslinger T., *Nature*, **483** (2012) 302.
[25] Kolovsky A. R. and Korsch H. J., *Phys. Rev. A*, **67** (2003) 063601.